

# COMPRESSIBILITY EFFECTS ON DISTRIBUTIONS OF PRESSURE AND LIFT COEFFICIENTS

Submitted on 01/02/2014 – Accepted on 28/09/2014

## Abstract

Reduce energy consumption of airplanes, or enhance the aerodynamic performance of compressors and turbines by reducing drag, or increasing lift is a major challenge for many institutions specializing in aerodynamics [1, 2]. One way to achieve this, is considered the study of compressible potential flow compared to incompressible potential flow [3], Outside the boundary layer, to study the effects of compressibility and the control parameters. And the pressure coefficient and lift distributions around the NACA 0012 profile, NACA 0015 and NACA 0018 were studied and presented in terms of the Mach number, angle of attack and the relative thickness of the profiles.

**Keywords :** *compressibilité, coefficient de pression, coefficient de portance*

**NAHOUI AZZEDINE** <sup>1</sup>

**BAHI LAKHDAR** <sup>2</sup>

<sup>1</sup> Faculty of Sciences, Department of Physics, Msila University, Algeria.

<sup>2</sup> Laboratory of Energetic Physics, Frères Mentouri University Constantine, Alegria.

## I. INTRODUCTION

The study of potential stationary compressible flow serves as data for modeling steady viscous flow, linearization of the mathematical model of the compressible flow potential through the transformation Prandtl-Glauert allowed to use incompressible flow potential, therefore, the mathematical model is only linearized by Laplace equation [4] with the tangency and Kutta-Joukowski conditions. The method adopted for the resolution of the flow is that of the panels that is widely used in this field. The results obtained allowed the positive effect of compressibility on the distributions of pressure and lift coefficients, which are been studied and shown with consideration of the effects of the Mach number, angle of attack and relative thickness profiles of NACA 0012, NACA 0015 et NACA 0018

## II. MATHEMATICAL MODELING

### II.1 - Compressible potential flow equation

The equation that manages the compressible flow potential is

$$(1 - M_\infty^2) \partial^2 \phi / \partial x^2 + \partial^2 \phi / \partial y^2 = 0 \quad (1)$$

With the following change

$$\beta^2 = 1 - M_\infty^2 \quad (2)$$

The equation (6) takes the form

$$\beta^2 \partial^2 \phi / \partial x^2 + \partial^2 \phi / \partial y^2 = 0 \quad (3)$$

In order to facilitate the resolution of equation (3), it is proposed to use the transformation Prandtl-Glauert which allows to linearize this equation, linearization allows the equation to take the form of the Laplace equation.

$$\nabla^2 \phi = 0 \quad (4)$$

## II.2. Boundary conditions

### II.2.1. Condition of tangency

This condition of tangency or condition of non penetration of fluid through each panel resulted in the invalidity of the normal velocity at each panel [4, 5 and 6] and is expressed by the system of equations

$$(v^n)_i = 0, \text{ avec } : i = 1, n \quad (5)$$

### II.2.2. Kutta-Joukowski condition

The Kutta condition-Joukowski is to use the tangential velocities at the panels forming the trailing edge and which is translated by the equation.

$$v_1^t = v_n^t$$

### II.2.3 Prandtl-Glauert transformation

The resolution of compressible potential flow problem is difficult, which is why we propose to spend compressible case difficult to relatively easy incompressible case through the transformation of Prandtl-Glauert, this transformation did involve changes coordinates of problem variables x, y and the potential  $\phi$  using equations

$$x_{incomp} = \beta x_{comp} \quad y_{incomp} = \beta y_{comp}$$

$$\phi_{incomp} = \beta^2 \phi_{comp}$$

These changes allow to linearize equation (3) in the form of the Laplace equation (8) which is relatively easy to solve. Once the rates obtained by the flow calculation in the incompressible landmark, we move at speeds in the compressible landmark by the following equations

$$u_{incomp} = u_{comp} / \beta^2$$

$$v_{incomp} = v_{comp} / \beta^2$$

Equations (4) and (5) for determining the pressure and lift distribution on the center of each panel. Thus, the flow is perfectly modeled in fact the mathematical model, which is that the Laplace equation or equation Laplace linearized [4, 5 and 6] with their boundary conditions.

### III. RESOLUTION MATHÉMATIQUE

The mathematical resolution is to discretize the mathematical model and the physical domain at a time by one of the discretization methods, the method most used in this area and that of the panels. This discretization allows the passage of the differential equation (3) the system of algebraic equations (12), which is solved by a direct numerical methods.

#### III.1. Discretization of the computational domain

The bearing surface is divided in to small segments called straight panels, plus the number of panels is important the closer you get the actual profile. The figure below shows an airfoil discrete [7].

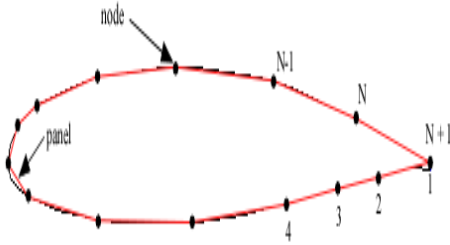


Fig. 1 Discretization of the bearing surface of n panels

On the panels are distributed sources of varying density from one panel to another and vorticity of constant density along the entire contour. Each panel is characterized by its orientation to the horizontal and has a length

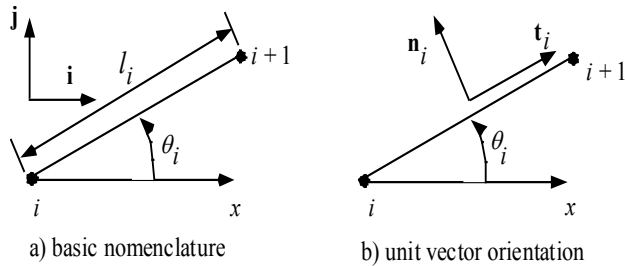


Figure 2 Local coordinate system of nomenclature

The unit vectors of the local system, the angle which the panel and length's, defined by the following equations

$$\vec{n}_j = -\sin \theta_j \vec{i} + \cos \theta_j \vec{j} \quad (6)$$

$$\vec{t}_j = \cos \theta_j \vec{i} + \sin \theta_j \vec{j} \quad (7)$$

$$\theta_j = \arcsin \left( \frac{y_{j+1} - y_j}{x_{j+1} - x_j} \right) \quad (8)$$

$$l_j = \sqrt{(x_{j+1} - x_j)^2 + (y_{j+1} - y_j)^2} \quad (9)$$

### III.2. Discretization of equations

#### III.2.1. Condition of non-permeability fluid

Under the condition of non-penetration of the fluid through the solid airfoil, the normal speed to the panels according to the equation is discretized

$$\sum_{j=1}^n [A_{ij}^n q_j] + \gamma \sum_{j=1}^n [B_{ij}^n] + U_\infty \sin(\alpha - \theta_j) = 0 \quad (10)$$

This system of equations containing  $n + 1$  unknowns, another equation is needed, is the reason why use is made of another additional condition which is that Kutta-Joukowski

#### III.2. Kutta-Joukowski condition

The Kutta condition Joukowski- led the following discrete equation

$$\sum_{j=1}^n [A_{ij}^t + A_{nj}^t] q_j + \gamma \sum_{j=1}^n [A_{ij}^t + A_{nj}^t] = U_\infty (\cos(\alpha - \theta_i) + \cos(\alpha - \theta_n)) \quad (11)$$

Equations (10) and (11) form a linear system of equations  $n + 1$  and  $n + 1$  unknowns expressed by

$$A_{ij} q_j = Rhs(j) \quad (12)$$

The system of equations (12) is linear and its resolution is obtained by a so-called direct digital methods with the definition of influence coefficients

$$A_{ij}^n = \frac{1}{2\pi} \left[ \sin(\theta_i - \theta_j) \ln \frac{r_{ij+1}}{r_{ij}} + \cos(\theta_i - \theta_j) \beta_{ij} \right] i \neq j$$

$$A_{ij}^t = \frac{1}{2\pi} \left[ -\cos(\theta_i - \theta_j) \ln \frac{r_{ij+1}}{r_{ij}} + \sin(\theta_i - \theta_j) \beta_{ij} \right] i \neq j$$

$$A_{ij}^n = \left[ \frac{1}{2} \right] i = j \quad A_{ij}^t = [0] i = j$$

$$B_{ij}^n = \frac{1}{2\pi} \left[ \cos(\theta_i - \theta_j) \ln \frac{r_{ij+1}}{r_{ij}} - \sin(\theta_i - \theta_j) \beta_{ij} \right] i \neq j$$

$$B_{ij}^t = \frac{1}{2\pi} \left[ \sin(\theta_i - \theta_j) \ln \frac{r_{ij+1}}{r_{ij}} + \cos(\theta_i - \theta_j) \beta_{ij} \right] i \neq j$$

$$B_{ij}^n = \left[ \frac{1}{2} \right] i = j \quad B_{ij}^t = [0] i = j$$

#### III.3. Digital Implementation of the panels method

1. The implementation of the method of the panels [8] allows calculation of the flow around the profiles of which the structure of the proposed program is
2. Declaration of data such as the speed at infinity, the angle of attack, Mach number and the number of panels
3. Once the geometry of the profile is chosen, a calculation of coordinates of each panel, calculating coordinates of

the center of each panel to which the parameters of the problem to be calculated, the corners of the panels with the horizontal and the length of each panel

4. Calculate the coefficients of the influence matrix and the vector constants of the equation system (12)
5. Resolution of the system of equations (12)
6. Calculation of the speed and pressure at the center of each panel and pressure and lift coefficients.
7. These coefficients contain  $r_{ij}$  and  $\beta_{ij}$  expressions that are defined by

$$r_{ij} = \sqrt{(xm_i - x_j)^2 + (ym_i - yx_j)^2}$$

$$\beta_{ij} = \arctg\left(\frac{ym_i - y_{j+1}}{xm_i - x_{j+1}}\right) - \arctg\left(\frac{ym_i - y_j}{xm_i - x_j}\right)$$

The right side of the equation is constant

$$RHS(j) = -V_\infty \sin(\alpha - \theta_j)$$

$$RHS(n+1) = V_\infty (\cos(\alpha - \theta_1) + \cos(\alpha - \theta_n))$$

### 3.2. Algorithm for calculating the compressible

- Discretize profile by dividing the contour into small segments (panels)
- Flatten the contour by applying processing Prandtl-Glauert contour
- Distribute singularities according to the profile bearing or non-bearing
- Discretize the equation of speed potential by applying the conditions of tangency and the Kutta-Joukowski
- Resolution of algebraic equations System.
- Obtaining axial and transverse velocities
- Calculation of axial and transverse velocities, application of the Prandtl-Glauert transformation.
- Calculation of the coefficient of pressure via the Bernoulli equation
- Lift coefficient calculation by using the pressure difference of the intrados and the extrados.

## IV. DISCUSSION OF RESULTATS

### IV.1. Distribution of the pressure coefficient

Compressibility effects are the essential part of this work, and their influences on the distributions of the pressure coefficient and lift coefficient. The effects of the Mach number, angle of attack and the relative thickness of the profile are also examined. The direct calculation is difficult; this is the reason why we use the transformation of the Prandtl-Glauert that allows the passage of the incompressible flow to compressible flow. These calculation steps are organized according to the above detailed calculation algorithm below.

#### IV.1.1 onset of compressibility effects

The distribution of the pressure coefficient does not depend on the Mach number in incompressible flow, but in

compressible flow, it is insensitive to the Mach number equal to or less than 0.4. When the Mach number is greater, the distribution of the pressure coefficient begins to appear some difference than that of the incompressible flow. The difference is even greater than the Mach number; this is only in the field of compressible subsonic flow [9].

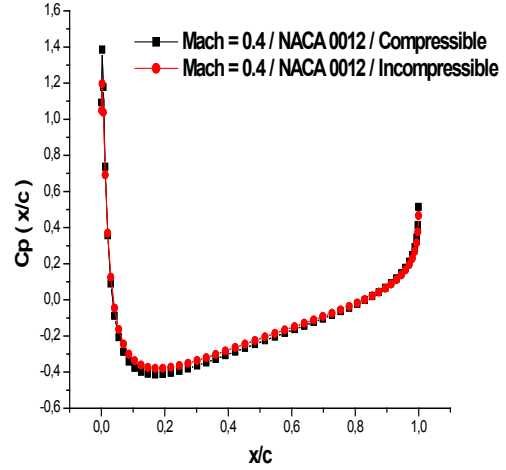


Fig. 3 Distribution of the pressure coefficient, NACA 0012, Mach = 0.4,  $\alpha = 0^\circ$

### IV.1.2. Effect of the Mach number on the pressure coefficient

The compressibility is manifested through depending on the number of pressure coefficient Mach, in effect, especially as the Mach number is large in the area of subsonic compressible, the pressure coefficient takes the minimum value point of the coefficient pressure further.

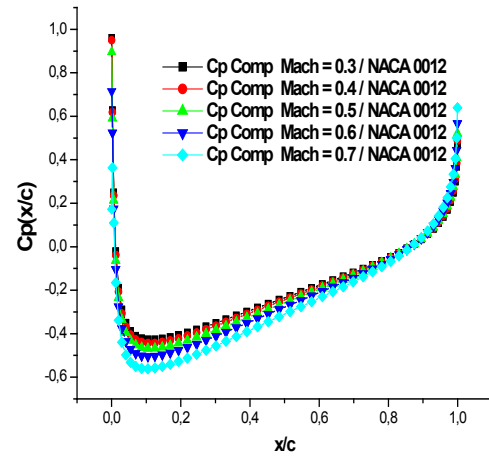


Fig. 4 Compressibility effects on the distribution of the pressure coefficient,  $\alpha = 0^\circ$

### IV.1.3. Effect of angle of incidence on the distribution of the pressure coefficient

For zero attack angle, the distribution of the pressure coefficient is the same on the lower surface on the upper surface for reasons of symmetry, but more the angle of attack, the greater the profile is asymmetrical manifest, therefore, the fluid particles are accelerated on the upper surface and the pressure decreases, but, on the pressure side, the fluid particles are decelerated gradually as the pressure increases,

therefore, this asymmetry is differentiating distribution pressure on both sides by creating a surface delimited by these distributions of pressure coefficients, which continues to increase as a function of the angle of attack. This area is bounded, in reality, a thrust upward force created following separate pressure difference across. This asymmetry also passed favorable flow velocity gradient and the negative gradient point of minimum pressure coefficient to advance the leading edge by promoting the separation of the boundary layer can be neglected beyond  $10^\circ$  [5] and the results will not be representative.

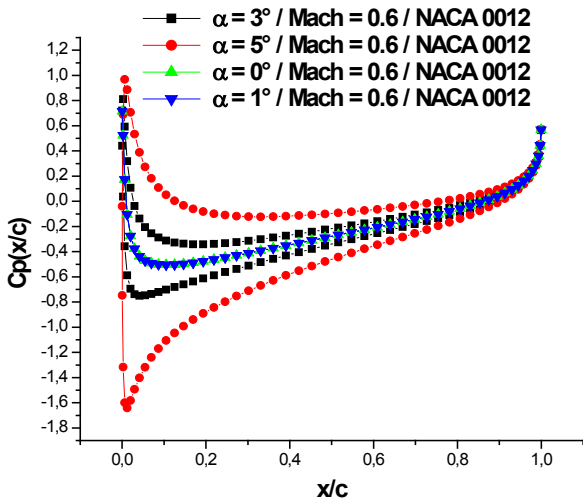


Fig. 5 Effect of angle of incidence on the distribution of the pressure coefficient, NACA 0012

**IV.1.4. Effect of the relative thickness of the distribution of the pressure coefficient**

A comparison of the distribution of the pressure coefficient around the NACA 0012 and NACA 0018 profiles for incompressible and compressible flows for zero attack angle and the Mach number given is made. This comparison shows that the relative thickness of the NACA 0018 profile offers more acceleration surface fluid particles the NACA 0012, so the pressure drops to a lower value depending on the importance of the thickness on increasing the lift coefficient and advancing the separation point

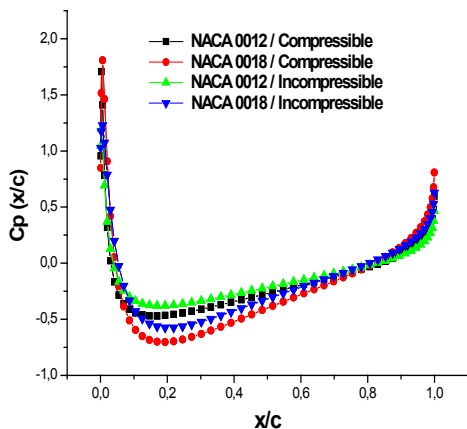


Fig. 6 Effect of the relative thickness of the profiles around NACA 00XX, Mach = 0.6,  $\alpha = 0^\circ$

**IV.2. Distribution of the lift coefficient of a compressible flow**

**IV.2.1. Compressibility effect on the distribution coefficient of lift**

As we saw in the paragraph above, the angle of attack was to create a kind of thrust upward force due to pressure difference on upper and lower surfaces [10], the coefficient of lift is only the result of this pressure difference. The distribution of the coefficient of lift as a function of angle around a NACA 0018 profile in incompressible flow potential is linear. Mach number influences the distribution of the lift coefficient via the coefficient of pressure, therefore, the higher the Mach number, the greater the lift coefficient is large.

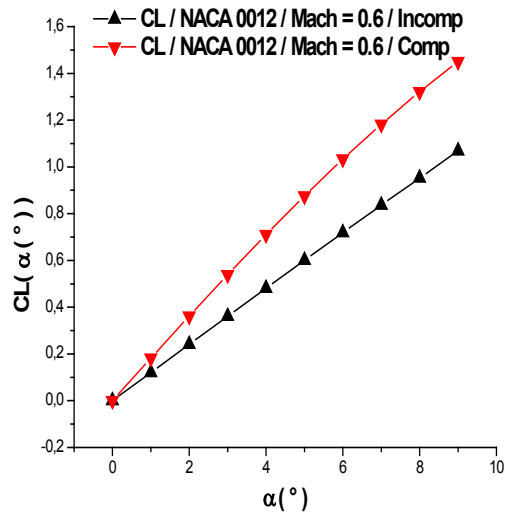


Fig. 7 Distribution of the lift coefficient, Mach = 0.6

**IV.2.2 The thickness effect on the distribution of lift coefficient**

The relative thickness of the profiles NACA 0012, 0015 and 0018 has no positive effect on the distribution of the coefficient of lift as a function of angle of attack, in fact, in the portion of the low angles of attack curve the agreement is total, but for angles strong values, the disagreement begins to manifest in favor of larger radius

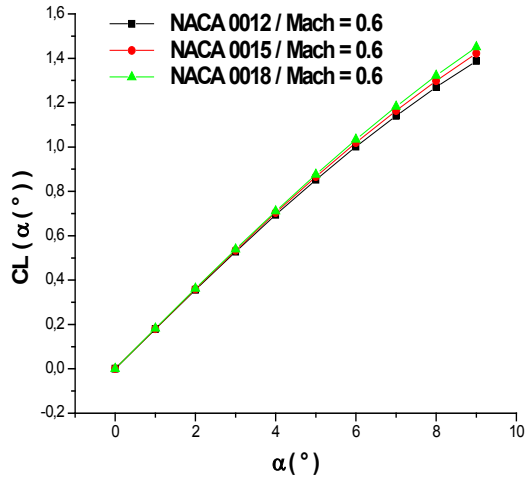


Fig.8 Effect of the relative thickness of the distribution of the lift coefficient around NACA 00XX

**IV.2.3. Effect of the Mach number on the lift distribution coefficient**

The Mach number has no positive effect on the lift coefficient distribution for the angle 0 °, the goal the greater angle of attack is wide, the effect becomes more and more significant for Mach number is greater. Therefore, compressibility has a positive effect on the distribution of the lift coefficient.

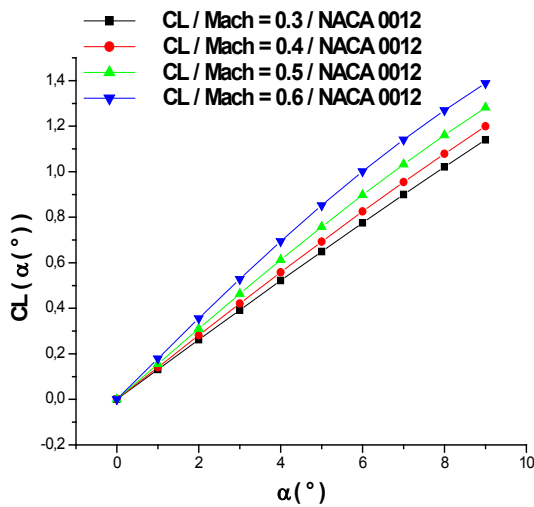


Fig.9 Effect of the Mach number on the distribution of the lift coefficient NACA 0012

**CONCLUSION**

A study of the potential compressible flow, is made digitally, based on the Laplace equation linearized mathematical whose resolution is based on the method the panels. The distributions of pressure coefficients and lift around the NACA 00XX type profiles were studied and presented. Mach number, angle of attack and the relative thickness of the profiles, were examined. Comparison between the processing flow of the incompressible and compressible flows, show the effect of the Mach number, the

main parameter of compressibility effects on the aerodynamic characteristics.

**REFERENCES**

- [1]. Corentin. Sainmont« Mémoire de Maitrisees sciences appliquées », Décembre 2009.
- [2]. Lagmich. Youcef, « Diagnostic etModélisationd’unedécharge à baterieélectrique pour le controle de l’écoulement », 29/11/2007.
- [3]. M.C. Cullagh and J. Nelder, « Subsonic Compressible Flow LinearTheory Java Vortex Panel Method », <http://www.engapplets.vt.edu>.
- [4]. Lisa M; nowak, «Computational Investigations of a NACA 0012 airfoil in low Reynolds Number, flows », Septembre 1992
- [5]. E. Foissac, B. Lerouyer, A. Meunier « Modélisation de la Méthode des Panneaux avec Tourbillons par Formulation de Linge de Courant». [www.oocities.org/dynabenja1/aerodynamique/aerodoc.htm](http://www.oocities.org/dynabenja1/aerodynamique/aerodoc.htm)
- [6]. Hess-Smith « Panel Method AA2000b, Lecture 3 », January 13-18,2005
- [7]. «Incompressible Potential Flow Using Panel Methods », [www.aoe.vt.edu/~mason/Mason\\_f/CAtxtChap4.pdf](http://www.aoe.vt.edu/~mason/Mason_f/CAtxtChap4.pdf)
- [8]. C.A.J Fletcher «Computational Techniques for Fluid Dynamics 2 », Ed 1991
- [9]. Kuethe and Chow «SubroutineLVFoil (XB,YB, n, alpha D, X, Y, Cp). Linearvorticity surface panel method for airfoils. », Ed 1991
- [10]. Steven D. Miller D.Miller Smiller «Lift, Drag and moment of a NACA 0015 Airfoil », Department of Aerospace engineering 28 May 2008.